AN EXPERIMENTAL AND NUMERICAL STUDY OF FLOW AND HEAT TRANSFER IN COOLING CHANNELS WITH PIN FIN-DIMPLE AND PIN FIN-GROOVE ARRAYS

V. Kindra[1] - S. Osipov[2] - D. Kharlamova[3] - I. Shevchenko[3]

National Research University "Moscow Power Engineering Institute"
14 Krasnokazarmennaya Street, 111250, Moscow, Russia
[1]Department of Thermal Power Plants
[2]Department of Steam and Gas Turbines
[3]Department of Innovative Technologies of High-Tech Industries
kindra.vladimir@yandex.ru - osipovsk@mail.ru - daria-rostov@yandex.ru - mmm@mati.ru

ABSTRACT

The study aims at improving the cooling design for the gas turbine components. A numerical and experimental study was conducted to investigate the heat transfer and the flow friction performance in rectangular channels with staggered arrays of pin fins, pin fin-dimples, where dimples located under the pin fins and pin fin-grooves, where the rows of pin fins located in grooves. The comparison based on the experimental data in the Reynolds number range of 4000–14000 showed that, compared with pin fin channel, the pin fin-dimple channel has increased convective heat transfer performance by about 11% and increased flow friction by 9%, the pin fin-groove channel has increased convective heat transfer performance by about 36% and decreased flow friction by 46%. In addition, numerical computations have been done to investigate the physical details about the flow and heat transfer in the pin fin-dimple and pin fin-groove channels. The computations showed that the dimples and grooves increase the near-wall turbulent mixing level by producing strong vortex flows around pin fins, and therefore enhance the convective heat transfer in the channel.

KEYWORDS

PIN FIN-DIMPLE, PIN FIN-GROOVE, STAGGERED ARRAY, GAS TURBINE COOLING

NOMENCLATURE

b channel wall thickness [mm]
B channel width [mm]
C_p specific heat capacity [kJ/(kg·K)]
D diameter [mm]
f linear hydraulic resistance coefficient [-]
F channel section area [m^2]
G massflow [kg/s]
H channel height [mm]
l channel characteristic length [mm]
L channel length [mm]
m_z zinc coat mass [kg]
N plate length [mm]
P pressure [Pa]
ΔP averaged pressure difference at the plate inlet and exit [Pa]
q heat flux density [W/m^2]
R_z zinc crystallization heat [kJ/kg]
S pitch [mm]
T temperature [°C]
U velocity [m/s]
Nu Nusselt number [-]
Re Reynolds number [-]
α heat transfer coefficient [W/(m^2·K)]
δ_z zinc coat thickness [mm]
η thermal-hydraulic efficiency coefficient [-]
λ thermal conductivity [W/(m·K)]
μ dynamic viscosity [Pa·s]
ρ density [kg/m^3]
τ blowing time [s]
CFD computational fluid dynamics
RMS root mean square
SST shear stress transport

INTRODUCTION

One of the main methods for convection heat transfer intensification is the flow turbulization over cooled surfaces. This method may be introduced by the location of ribs, pin fins, and dimples on coolant blown surfaces (Han et al., 2012). The method increases the heat transfer by swirl-translational flow motion and decay of wall flow layers (Nazmeev, 1998).

The heat transfer intensification in a channel with a dimple is related to the formation of conical swirls that suck the boundary layer from the dimple bottom and adjoined channel surface (Kovalenko et al., 1980). The heat transfer increase by the surface dimples introduction is considerably determined by the dimple shape, geometry parameters and flow motion mode (Isaev and Leontiev, 2003; Kovalenko et. al, 2010; Kinkadze et. al, 2012).

Pin fin array remarkably increases the cooled surface area. The main heat transfer intensification zone is located in the turbulator frontal part, but in its "shadow" zone there is a separation zone with low heat transfer coefficients. Staggered pin fin arrays are often used for heat transfer increase in cooling channels internal surface of gas turbine blades trailing edge. As the result, the Nusselt number values may be about two times increased (Metzger et. al, 1982).

In recent years especially actual are investigations of various pin fin and dimple turbulator combinations intended for heat transfer intensification (Xie et. al, 2017; Rao et. al, 2012).

This report presents results of numerical and experimental investigations of thermal-hydraulic processes of three cooling channels with different flow turbulization systems: the pin fin array (the datum version), the pin fin-dimple array pluck swirls (the first developed version) and pin fin-groove array (the second developed version). In addition, the physical details about the flow and heat transfer in the considered channels are described. Finally, it is concluded that the dimples and grooves increase the near-wall turbulent mixing level by producing strong vortex flows around pin fins, and therefore enhance the convective heat transfer in the channel.

PROMISING MODIFICATIONS OF THE STAGGERED ARRAYS OF PIN FINS

Cooling Channels Geometric Parameters

The investigated models are rectangular cross-section channels with H=2 mm height, B=15 mm width, L=55 mm length and b=2.5 mm wall thickness with three turbulator versions, staggered pin fin array, staggered pin fin-dimple array and staggered pin fin-groove array. The turbulator location scheme and its main dimensions are shown in figure 1.

Pin Fin Array

The first version considered is the staggered pin fin array. This version makes a basis for comparison with the heat transfer performance of other versions. The array consists of eight pin fin rows installed at 90° angle to the channel wall (figure 1a). The pin fin diameter D_{pin}=2 mm is compatible with this type turbulators in blade trailing edges. The longitudinal and transversal pitch to pin fin diameter ratios S_1/D_{pin} and S_2/D_{pin} are assumed 2.5 that corresponds to maximal heat transfer intensity in staggered pin fin arrays (Han et al., 2012). The channel height to pin fin diameter ratio is assumed H/D_{pin}=1, which corresponds to the cooled blades trailing edge actual dimensions (Metzger et. al, 1982).

Pin Fin-Dimple Array

The first modification of the pin fin array is the pin fin-dimple array. The pin fin-dimple is representing the spherical dimple on the channel surface with pin fin co-axially placed in it (Kindra et.al, 2017a). This type of flow turbulators is presented in figure 1b. The dimple diameter D_{dimp} and depth H_{dimp} are taken from the channel thermal-hydraulic performance computer simulation described in the next chapter.

The computer simulation comparison of different single turbulators (Kindra et. al, 2017b) shows that at Reynolds numbers from 8000 to 70000 a pin fin-dimple turbulator provides 7-13% higher Nusselt numbers than a single pin fin.

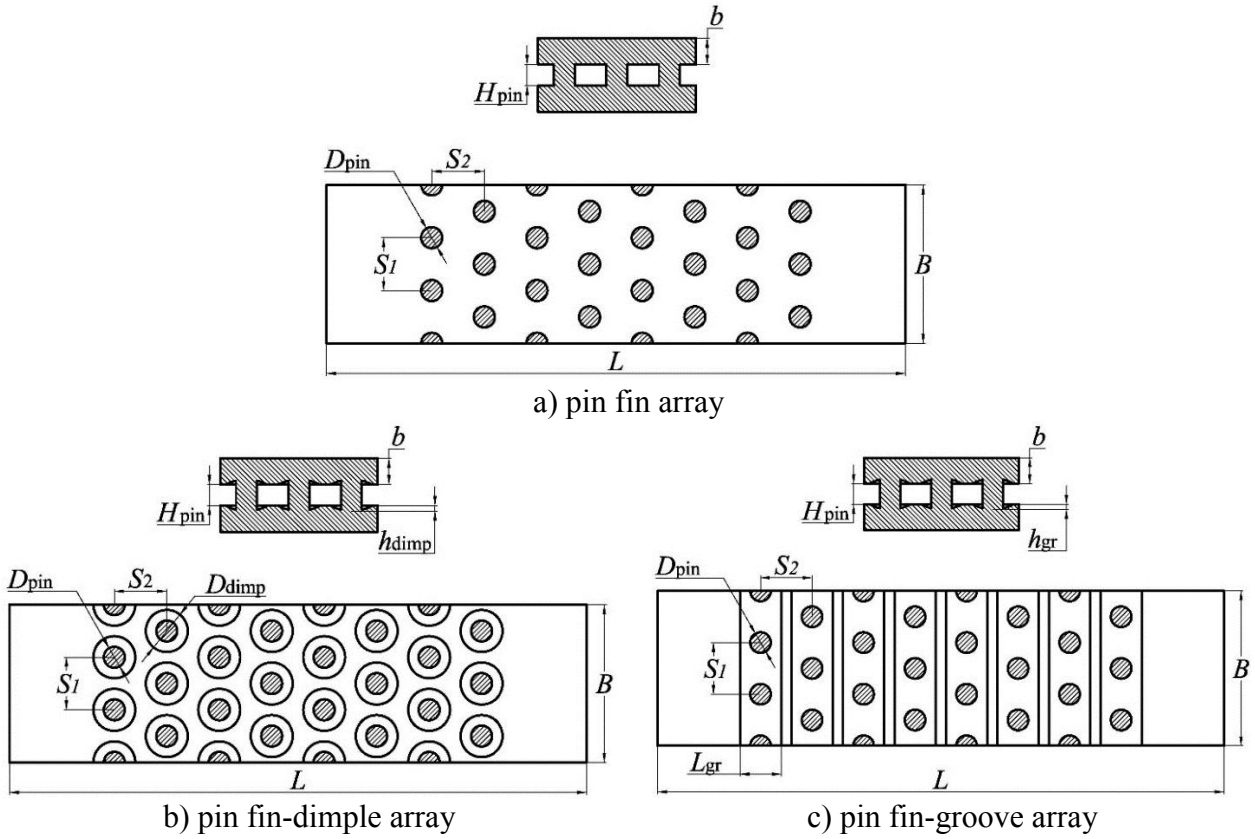

Figure 1: Cooled channels with staggered arrays of flow turbulators

Nowadays it is difficult to apply the pin fin-dimple arrays in blade trailing edges because the current precise casting technology does not allow the introduction of this technical solution. Nevertheless, it is possible to hope that the intensive technology improvements will soon provide a solution to this problem.

This type of flow turbulators also may be applied to various heat exchange facilities and cooling channels. Specifically, the pin fin-dimple principle may be prospective for tubular-plate heat exchangers. In this case, the tubes are pin fins and the plate surface around the tube connections may have specific spherical dimples.

Pin Fin-Groove Array

The problem of trailing edge manufacturing with the pin fin-dimple array directed the development of a pin fin-groove array – the staggered pin fin array with pin fin rows placed in transversal grooves. A gas turbine blade with this flow turbulization system may be manufactured by the lost wax casting.

The developed flow turbulator location scheme is shown in figure 1c. The dimensions like the groove length L_{gr} and depth h_{gr} are taken according to computer performance optimization disclosed in the next chapter.

NUMERICAL SIMULATION OF THERMAL-HYDRAULIC PROCESSES IN COOLING CHANNELS WITH DIFFERENT FLOW TURBULATORS

Problem Definition and Simulation Method

The heat transfer problem is solved in a combined approach including cross-influence of the coolant flow and channel wall metal.

The channel wall mesh is tetrahedral unstructured with the element maximal linear dimension of 0.5 mm. The total number of tetrahedral elements for different models is 3.6 to 3.8 million.

The flow simulation meshes are hybrid unstructured. The main flow zone is formed of tetrahedrons, the wall zone of prisms. The main flow element maximal linear dimension is 0.2 mm, the total elements number is 6.7 to 7.0 million.

The results of the mesh sensitivity analysis showed that the acceptable number of the prism layers is 13, while the initial height of the first prism layer is 0.0015 mm. The acceptable main flow element size is 0.75 mm.

At the channel inlet was given the air massflow that controls the Reynolds number values from 20000 to 80000 and the total air temperature of 20 °C. The channel exit constant pressure was atmospheric.

The channel outer wall temperature T_{wall}=419 °C, which is equal to the zinc crystallization on the model outer wall at the surface temperature (Shevchenko et. al, 2018). The wall material heat conductivity λ is 16 W/(m·K). The side walls of the channels were treated as periodic. The Reynolds averaged Navier-Stocks equations were closed with the SST turbulence model. The y^+ is less than 1 for all Reynolds numbers investigated. The simulation actual air parameters correspond to the data by (Vargaftik, 1963). The thermal-hydraulic process simulation is carried out with Ansys CFX code.

Method for Thermal-Hydraulic Efficiency Analysis

The channel internal surface blown with the air flow is split into 5 mm wide transversal plates. Each plate includes one row of pin fins (figure 2).

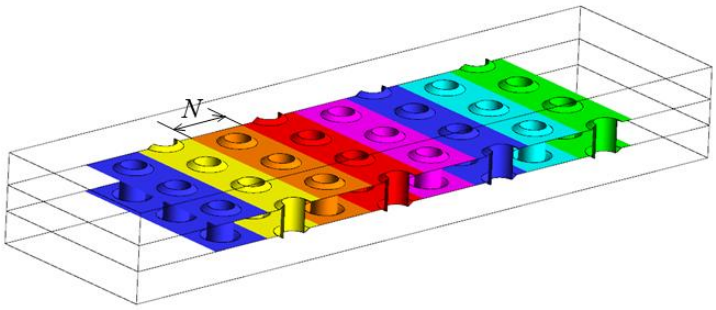

Figure 2: The channel internal surface split into plates

The Nusselt number for the *i*-th plate was defined as follows (1):

$$\mathrm{Nu}_i = \frac{\alpha_i \cdot l}{\lambda_i}. \tag{1}$$

The heat transfer coefficient for the *i*-th plate α_i was estimated by the ratio of heat flux density for the *i*-th plate q_i to the difference between area average wall temperature for the *i*-th plate $T_{wall.i}$ and reference temperature $T_{air.i}$. The pin fin diameter D_{pin} was assumed as the characteristic length l. The reference temperature was average bulk air temperature for the *i*-th plate.

The *i*-th plate Reynolds number was defined as follows (2):

$$\mathrm{Re}_i = \frac{G \cdot l}{\mu_i \cdot F}. \tag{2}$$

The *i*-th plate linear hydraulic resistance coefficient was defined as follows (3):

$$f_i = \frac{\Delta P_i \cdot l}{2 \cdot \rho_i \cdot (U_i)^2 \cdot N}, \tag{3}$$

where plate length N is 5 mm (figure 2), averaged pressure difference ΔP_i is the difference between area averaged pressures at the plate inlet and exit.

The channel mean Nusselt number Nu_{aver}^{turb}, the channel mean linear hydraulic resistance coefficient f_{aver}^{turb}, and the channel mean Reynolds number Re_{aver}^{turb} were determined as the arithmetic mean for all plates.

Thermal-hydraulic efficiency coefficient of the channel was defined as follows (4):

$$\eta_{aver} = \frac{Nu_{aver}^{turb} / Nu_{aver}^{0}}{\left(f_{aver}^{turb} / f_{aver}^{0} \right)^{1/3}}, \quad (4)$$

where Nu_{aver}^{0} represents mean Nusselt number in a smooth channel; f_{aver}^{0} represents mean linear hydraulic resistance coefficient in a smooth channel.

Influence of Flow Turbulator Dimensions upon the Cooling Channel Thermal-Hydraulic Performance

The study and analysis goal was to determine the turbulator geometry parameters applicable to the heat transfer intensification in blade trailing edges based on the results of the numerical modeling.

The pin fin-dimple turbulator efficiency parameters were the following:

- the ratio of average Nusselt number values for pin fin-dimple and pin fin arrays Nu_{pfd}/Nu_{pf};
- the ratio of average linear hydraulic resistance coefficients for pin fin-dimple and pin fin arrays f_{pfd}/f_{pf};
- the ratio of thermal-hydraulic effectiveness coefficients for pin fin-dimple and pin fin arrays η_{pfd}/η_{pf}.

Figure 3 shows the influence of the specific pitch diameter D_{dimp}/D_{pin} from 1.5 to 2.5 and the specific pitch depth H_{dimp}/D_{pin} from 0.25 to 0.5 on the parameters above. Relations in the figure are results of parameters averaging at Reynolds number values from 20000 to 80000 with Reynolds number step of 10000. In other words, each point on the plots represents the average value of 7 cases corresponding different Reynolds numbers.

Increases of the dimple depth H_{dimp}/D_{pin} from 0.25 to 0.5 and diameter D_{dimp}/D_{pin} from 1.5 to 2.3 causes growth of the Nu_{pfd}/Nu_{pf} and f_{pfd}/f_{pf} ratios (figure 3a and figure 3b) but the hydraulic resistance changes are not quite distinct (figure 3c).

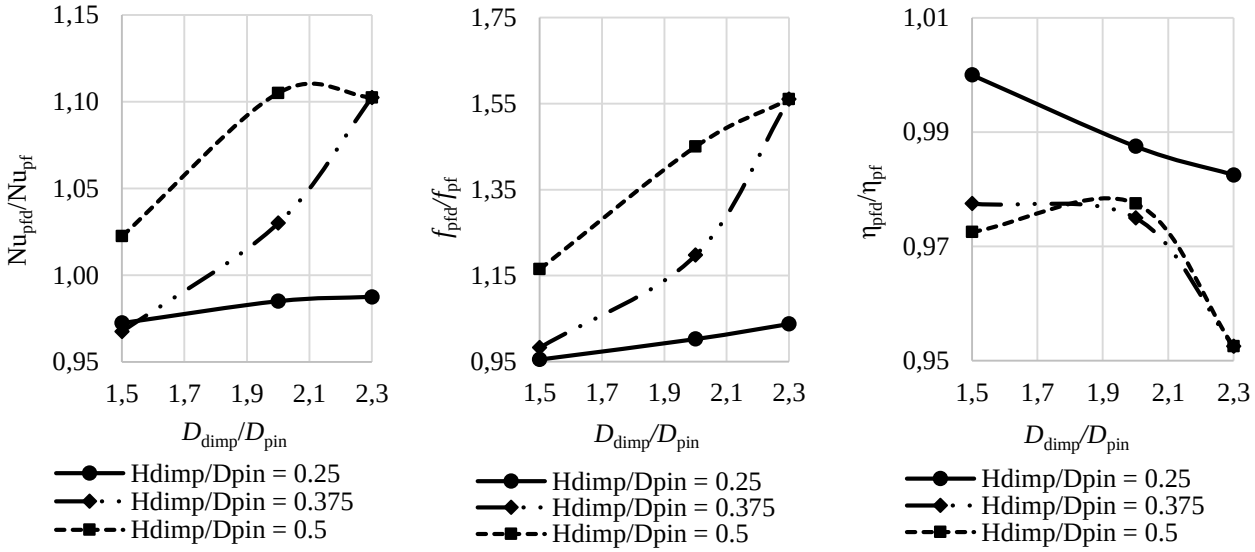

a) heat transfer performance b) hydraulic performance c) thermal-hydraulic performance

Figure 3: Influence of pin fin-dimple geometry parameters upon the channel thermal-hydraulic performance (numerical modeling results)

The maximal 1.11 increase of the ratio Nu_{pfd}/Nu_{pf} is reached at the dimple specific diameter 2.0 and depth 0.5. Thus any further increase of the dimple diameter above 2.0 is not reasonable. These parameters correspond to the channel hydraulic coefficient of 1.45 and thermal-hydraulic coefficient of 0.99.

An influence of the groove relative length L_{gr}/D_{pin} from 1.5 to 2.0 and depth H_{gr}/D_{pin} from 0.25 to 0.5 on the channel thermal-hydraulic performance is presented in figure 4 (here L_{gr}/D_{pin}=2.0 dimension corresponds to the maximal manufacturing capability). The research method for pin fin-groove array was the same as for pin fin-dimple array.

The groove relative depth H_{gr}/D_{pin} increase from 0.25 to 0.5 is followed by a remarkable growth of Nu_{pfg}/Nu_{pf} and f_{pfg}/f_{pf} (figure 4a and figure 4b) and drop of η_{pfg}/η_{pf} (figure 4c) ratios.

The maximal increase of Nu_{pfg}/Nu_{pf} equal to 1.07 is reached at the groove relative length of 2.0 and depth of 0.5. At these parameter values, the channel hydraulic and thermal-hydraulic coefficients are 1.44 and 0.86 respectively.

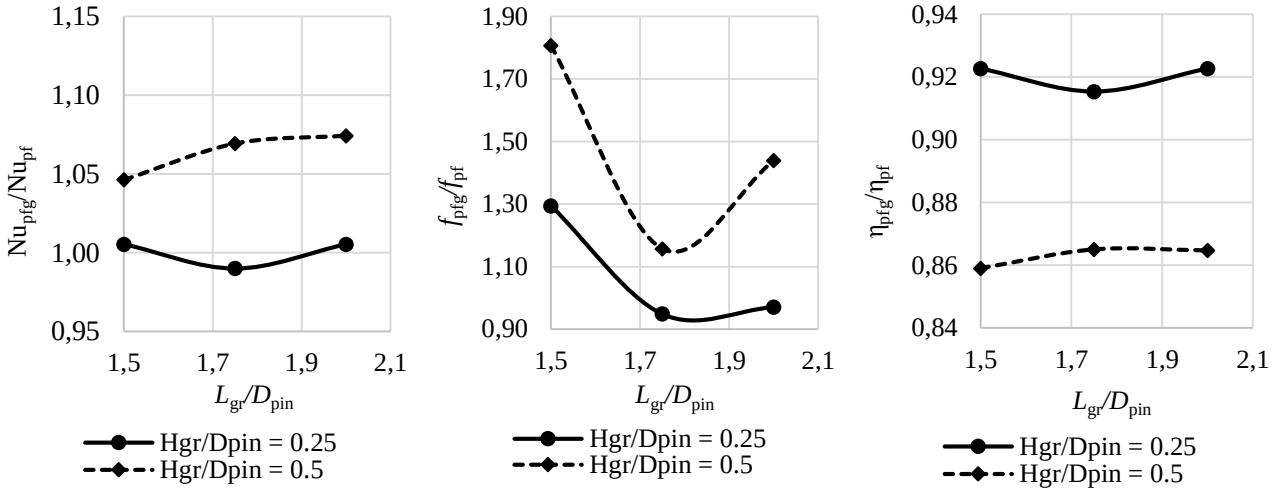

a) heat transfer performance b) hydraulic performance c) thermal-hydraulic performance

Figure 4: Influence of pin fin-groove geometry parameters upon the channel thermal-hydraulic performance (numerical modeling results)

The variation of Reynolds numbers in the range of 20000-80000 may result in maximum results deviation (compare to average values presented on the figures 3 and 4) by 3-6% for ratios Nu_{pfd}/Nu_{pf} and Nu_{pfg}/Nu_{pf}, 14-36% for f_{pfd}/f_{pf} and f_{pfg}/f_{pf}, 5-12% for η_{pfd}/η_{pf} and η_{pfg}/η_{pf}.

The further analysis is carried out for the dimensions that provide maximal heat transfer intensity: dimple relative diameter and depth of 2.0 and 0.5, groove relative length and depth of 2.0 and 0.5.

The pin fin-dimple array intensive heat transfer is produced by the following. Near the frontal zone of a pin fin surface some flow is re-directed into a dimple (figure 5b), the flow axial velocity drops to zero and then changes the direction. The dimple frontal zone forms intensive swirl flow. The remarkable pressure drop between the frontal and rear dimple parts forms the swirl flow axial velocity that propagates along the whole dimple surface. As the result, this zone has maximal heat transfer and the stagnation zone downstream pin fin is absent.

Grooves in pin fin channels form confusor-diffuser channels in transversal planes where the flow in the near-wall zone intensively mixes and the boundary layer disintegrates (figure 5c).

The heat flux distribution along the channel outer surface presented in figure 6 confirms the conclusion above. For the pin fin turbulator case, the heat flux maximum is located in the frontal pin fin zone and the "shadow" zone (figure 5a) has lower heat transfer (stagnation zone). Application of pin fin-dimple turbulators and pin fin-groove turbulators eliminates the stagnation zones and increases heat transfer over the whole turbulators surface.

These results are verified with the developed turbulator test described in the next chapter.

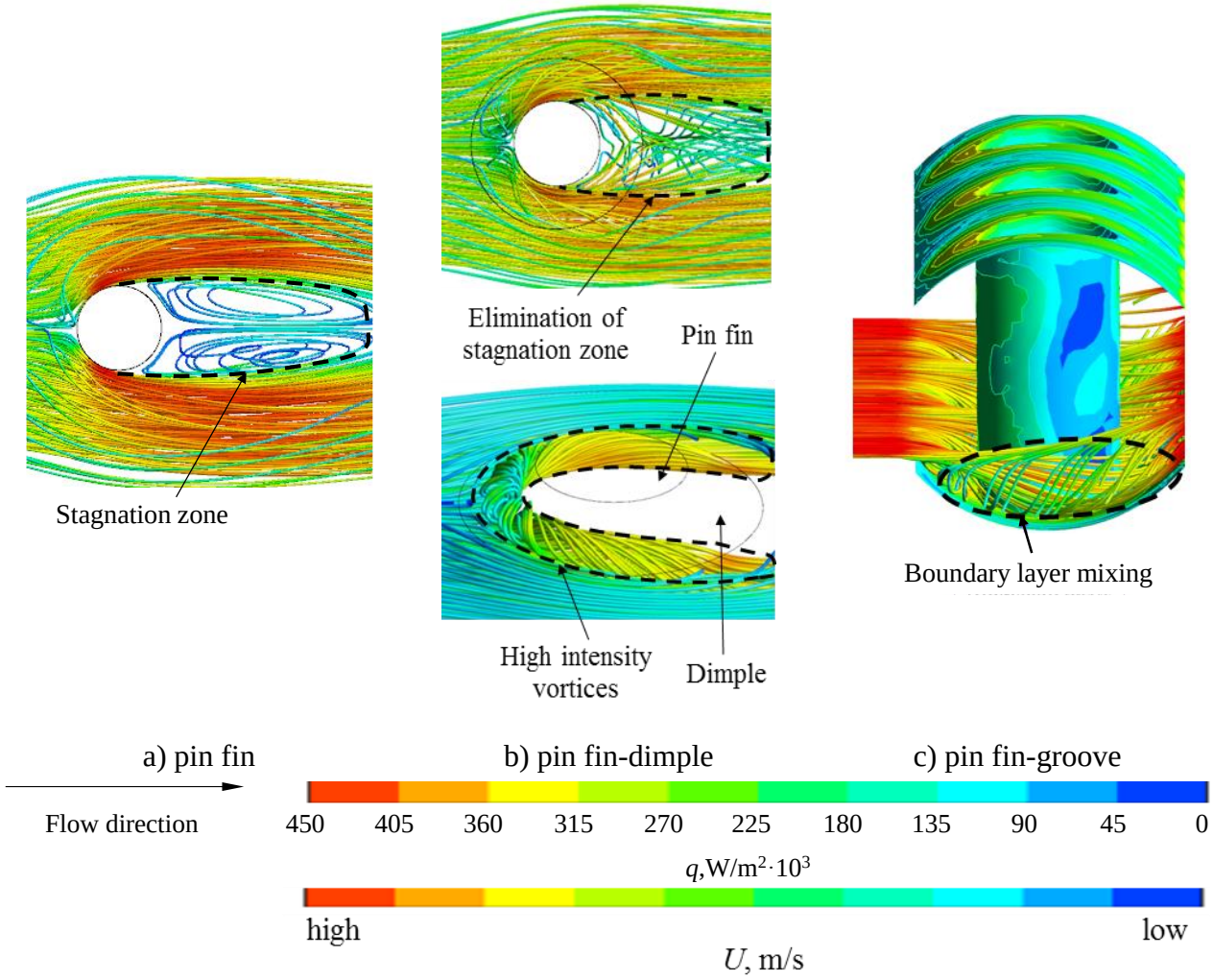

Figure 5: Streamlines around different turbulators

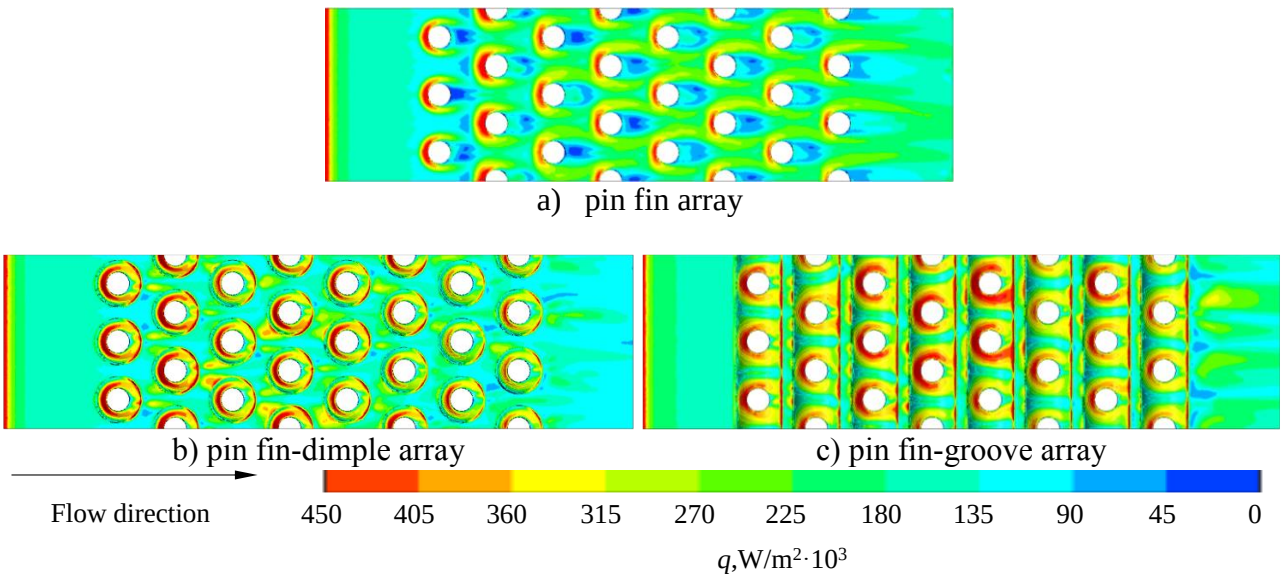

Figure 6: Distributions of heat flux in channels with different intensifier types, Re=40000

EXPERIMENTAL INVESTIGATION OF THERMAL-HYDRAULIC PROCESS IN CHANNELS WITH DIFFERENT FLOW TURBULATORS

Method of Calorimetric Measurement in the Liquid-Metal Thermostat

This method allows experimental measurement of local heat flow density values in each point of a closed cooling channel (Shevchenko et. al, 2018). An effect of phase transition of chemically pure metals is a physical basis of calorimetric method. The method proceeds as follows. A cooling channel equipped with manifolds for supply and extraction of cooling air shall be submerged into the melt of pure zinc heated over its melting point. The cooling channel shall be heated to the temperature of melt and then cooled along with it down to the equilibrium state at zinc melting point and blew by the cooling air within a particular period of time. After that, the cooling channel shall be taken out of the melt. A metal coat formed during the process of heat transfer to the coolant passing through the channel is crystallised on its outer surface. The thickness of the coat unambiguously characterizes the heat exchange intensity.

The following parameters are measured: air consumption through the cooling channel, incoming and outgoing air temperatures. After a series of experiments, zinc coats removed from the studied channel shall be weighted, which is necessary for evaluation of the quality of experiments with respect to convergence of thermal balance.

The thermal balance is defined as follows (5):

$$G \cdot C_p \cdot \left(T_{\text{in}} - T_{\text{out}}\right) = \frac{m_z}{\tau} \cdot \text{R}_z, \tag{5}$$

where T_{in} represents measured temperature of air incoming to the cooling channel, ℃; T_{out} represents measured temperature of air outgoing from the cooling channel, ℃.

Coats shall be marked and cut with respect to sections accepted for the study. Zinc coat images enlarged by 8 to 10 times shall be obtained by scanning. The use of enlarged images allows for essential improvement of accuracy of coat thickness measurement.

The heat flux density for the *i*-th calculation point is defined as follows (6):

$$q_i = \frac{\rho_z \cdot \text{R}_z \cdot \delta_{zi}}{\tau}, \tag{6}$$

where ρ_z represents the density of zinc coat, kg/m^3.

The heat transfer coefficient for the *i*-th calculation point is defined as follows (7):

$$\alpha_i = \frac{q_i}{\left(T_z - T_i\right)}, \tag{7}$$

where T_z represents zinc meting point, ℃; T_i represents air local temperature, ℃.

Different Turbulator Test Results Analysis

The tests were carried out with the following three channel models with different flow turbulators: staggered pin fin array (model B1), staggered pin fin-dimple array (model B2), staggered pin fin-groove array (model B3). All geometric parameters of the considered experimental models (B1, B2 and B3) correspond with parameters presented on the figure 1 with the exception of chanel width *B*, which is two times higher for experimental models in order to decrease the channel side walls influence on flow: H=2 mm, B=30 mm, L=55 mm, b=2.5 mm, S_1=S_2=5 mm, D_{pin}=2 mm, D_{dimp}=L_{gr}=4 mm and h_{dimp}=h_{gr}=1 mm.

The blow test results are shown in figure 7a. Model B2 has a larger flow path area than B1 but its flow capacity is smaller. The models B1, B2 and B3 flow path areas F in the pin fin row section are

36 mm^2, 41.14 mm^2 and 54 mm^2 respectively. The B3 mass flow is 45% larger than the B1 one at P/P_0=1.6, temperature factor T_{wall}/T_{air_mean}=2.3-2.5. Here P and P_0 are the model inlet and exit pressures; T_{wall} and T_{air_mean} are channel wall and channel mean air temperature.

The pin fin diameter D_{pin} is assumed as the specific dimension in Nusselt number and Reynolds number calculation. The reference temperature was mean air temperature T_{air_mean}.

The models heat transfer performance at Reynolds number 4000–14000 range show 11% Nu increase for the pin fin-dimple intensifiers and a 36% for the pin fin-groove intensifiers (figure 7b). The number equations for mean Nusselt values along the intensifier zone are calculated by RMS method. In the model B1 with pin fin array the equation is $Nu_{pf}=0.245\cdot Re^{0.6}$, in the model B2 with pin fin-dimple array – $Nu_{pfd}=0.271\cdot Re^{0.6}$ and in the model B3 with pin fin-groove array – $Nu_{pfd}=0.332\cdot Re^{0.6}$. The pin fin-groove array shows the maximal heat exchange intensity.

The staggered pin fin array (model B1) thermal performance is in a good correspondence with the test data (Metzger et. al, 1982) for relatively high Reynolds numbers such as 6000<Re<14000. The highest discrepancy, which is lower than 12%, is observed for low Reynolds numbers such as 4000<Re<5000. The highest values of Nusselt numbers are achieved for the third row of the pin fin array. The discrepancy between numerical and experimental results obtained in the study is not higher than 7%.

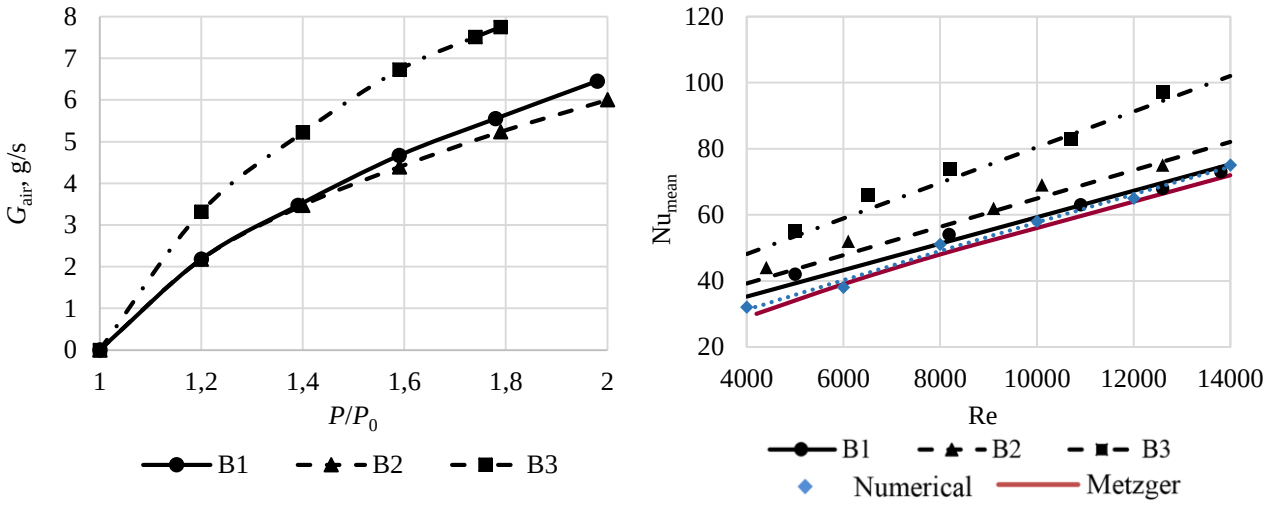

a) channels flow capacity performance b) channels heat transfer performance

Figure 7: The results of experimental investigation of the cooling channels with different flow turbulators (B1, B2 and B3 – experimental results for models B1, B2 and B3, Numerical – numerical results for model B1, Metzger – experimental results provided in (Metzger et. al, 1982) for model B1)

CONCLUSIONS

Two modifications of pin fin flow turbulators are being developed to intensify heat transfer in slot channels: the pin fin-dimple and the pin fin-groove. Computer studies show the flow turbulator dimensions for maximal heat transfer intensity.

For the staggered pin fin-dimple array with 2 mm pin fin diameter and 5 mm transversal and longitudinal pitch may be recommended a dimple of 4 mm diameter and 1 mm depth. Computer studies of this pin fin-dimple modification show an 11% heat transfer increase from the staggered pin fin array.

For the staggered pin fin-groove array with 2 mm pin fin diameter and 5 mm transversal and longitudinal pitch may be recommended application of a 4 mm long and 1 mm deep groove. Computer studies of this modification show a 7% heat transfer increase from the staggered pin fin array.

Numerical simulation shows streamlines with swirled streams formed in dimples around the pin fins frontal part of the pin fin-dimple flow turbulators. The streams propagate along the whole dimple

surface around pin fins and intensify the heat transfer. The streamlines computer analysis shows an intensive flow mixing in grooves that intensifies the heat transfer for the pin fin-groove array.

Numerical studies of the heat flux density in these three channel modifications show elimination of the "shadow" stagnation zone and high heat flux around pin fins in pin fin-dimple and pin fin-groove arrays.

The calorimetry in liquid metal thermostat test shows the minimal flow capacity for the channel with the pin fin-dimple array and maximal capacity for the channel with pin fin-groove array.

The tests show an 11% Nusselt number increase for the channel with pin fin-dimple array and a 36% increase for the channel with pin fin-groove array from the channel with pin fin array at Reynolds numbers from 4000 to 14000. (Here the Nusselt number is taken as average along the channel length.)

The investigation results are formulated as criterial equations that provide a calculation of the heat transfer coefficient with ±8% error.

ACKNOWLEDGEMENTS

This study conducted by National Research University "Moscow Power Engineering Institute" was supported by the Ministry of Education and Science of the Russian Federation (project No. 13.7616.2017/8.9).

REFERENCES

Han, J.C., Dutta, S., Ekkad, S., (2012). *Gas turbine heat transfer and cooling technology*. London: CRC Press, p. 843.

Nazmeev, J.G., (1998). *Laminar flow heat transfer in discretely uneven channels*. Moscow: Energoatomizdat, p. 372.

Kovalenko, A.N., Lebedev, A.S., Safonov, L.P., (1980). *Cooling of gas turbine airfoil*. Power machinery, 3 (4), 1-38.

Isaev, S.A, Leontiev, A.I., (2003). *Numerical simulation of vortex enhancement of heat transfer under conditions of turbulent flow past a spherical dimple on the wall of a narrow channel*. High Temperature, 41 (5), 665-679.

Kovalenko, G.V., Terekhov, V.I., Khalatov, A.A., (2010). *Flow modes in a single dimple located on channel surface*. Applied mechanics and technical physics, 51 (6), 78-88.

Kiknadze, G.I., Gachechiladze, I.A., Barnaveli, T.T., (2012). *The mechanisms of the phenomenon of torn ado-like jets self-organization in the flow along the dimples on the initially flat surface*. Proceedings of the ASME International Mechanical Engineering Congress and Exposition. Houston, Texas, USA.

Metzger, D.E., Berry, R.A., Bronson, J.P., (1982) *Developing heat transfer in rectangular ducts with staggered arrays of short pin fins*. Journal of Heat Transfer, 104 (4), 700-706.

Xie, Y., Shi, D., Shen, Z., (2017). *Experimental and numerical investigation of heat transfer and friction performance for turbine blade tip cap with combined pin-fin-dimple protrusion structure*. International Journal of Heat and Mass Transfer, 104, 1120-1134.

Rao, Y., Xu, Y., Wan, C., (2012). *An experimental and numerical study of flow and heat transfer in channels with pin fin-dimple and pin fin arrays*. Experimental Thermal and Fluid Science, 38, 237-247.

Kindra, V.O., Osipov, S.K., Lisin, E.M., Egorov, A.A., (2017a). *Developed heat transfer surface*, RF patent 2017113376, 18.04.2017.

Kindra, V.O., Osipov, S.K., Egorov, A.A., Schevchenko, I.V., Rogalev, A.N., (2017b). *Investigation and development of pin-dimple a heat transfer intensifier for high efficiency heat exchanging devices*. New in Russian power sector, 9, 76-89.

Shevchenko, I., Rogalev, N., Rogalev, A., Vegera, A., Bychkov, N., (2018). *Verification of Thermal Models of Internally Cooled Gas Turbine Blades*. International Journal of Rotating Machinery, 2018, 6780137.

Vargaftik, N.B., (1963) *Thermo-physical gas properties*. Moscow: Ripol Classic, p. 721.